



Article

Effect of Pulse Repetition Rate on Ultrafast Laser-Induced Modification of Sodium Germanate Glass

Sergey V. Lotarev ^{*}, Sergey S. Fedotov , Alyona I. Pomigueva, Alexey S. Lipatiev and Vladimir N. Sigaev

Department of Glass and Glass-Ceramics, Mendeleev University of Chemical Technology, Miusskaya pl. 9, 125047 Moscow, Russia; fedotov.s@muctr.ru (S.S.F.); pomigueva_a_i@muctr.ru (A.I.P.); lipatievas@muctr.ru (A.S.L.); vlad.sigaev@gmail.com (V.N.S.)

* Correspondence: sergeylo@gmail.com

Abstract: We report an unexpected pulse repetition rate effect on ultrafast-laser modification of sodium germanate glass with the composition $22\text{Na}_2\text{O} \cdot 78\text{GeO}_2$. While at a lower pulse repetition rate ($\sim < 250$ kHz), the inscription of nanogratings possessing form birefringence is observed under series of 10^5 – 10^6 pulses, a higher pulse repetition rate launches peripheral microcrystallization with precipitation of the $\text{Na}_2\text{Ge}_4\text{O}_9$ phase around the laser-exposed area due to the thermal effect of femtosecond pulses via cumulative heating. Depending on the pulse energy, the repetition rate ranges corresponding to nanograting formation and microcrystallization can overlap or be separated from each other. Regardless of crystallization, the unusual growth of optical retardance in the nanogratings with the pulse repetition rate starting from a certain threshold has been revealed instead of a gradual decrease in retardance with the pulse repetition rate earlier reported for some other glasses. The repetition rate threshold of the retardance growth is shown to be inversely related to the pulse energy and to vary from ~ 70 to 200 kHz in the studied energy range. This effect can be presumably assigned to the chemical composition shift due to the thermal diffusion of sodium cations occurring at higher pulse repetition rates when the thermal effect of the ultrashort laser pulses becomes noticeable.

Keywords: sodium germanate glass; nanograting; form birefringence; laser-induced crystallization; ultrashort laser pulses



Citation: Lotarev, S.V.; Fedotov, S.S.; Pomigueva, A.I.; Lipatiev, A.S.; Sigaev, V.N. Effect of Pulse Repetition Rate on Ultrafast Laser-Induced Modification of Sodium Germanate Glass. *Nanomaterials* **2023**, *13*, 1208. <https://doi.org/10.3390/nano13071208>

Academic Editor: Werner Blau

Received: 4 February 2023

Revised: 12 March 2023

Accepted: 21 March 2023

Published: 29 March 2023



Copyright: © 2023 by the authors. Licensee MDPI, Basel, Switzerland. This article is an open access article distributed under the terms and conditions of the Creative Commons Attribution (CC BY) license (<https://creativecommons.org/licenses/by/4.0/>).

1. Introduction

Nanogratings, often referred to as Type-II-fs modifications, are self-organized bulk nanoperiodical structures often regarded as the most intriguing ultrafast laser-induced phenomena in dielectric materials. This type of micromodification has become the first example of a regular sub-wavelength structure inscribed by optical methods inside homogeneous dielectrics [1]. A detailed investigation of the structure of nanogratings in fused silica showed that they consisted of parallel nanolayers (“nanoplanes”) possessing a reduced density and refractive index because of the presence of oxygen-filled nanopores separated with thicker layers of solid glass [2]. Due to nanoperiodic refractive index variation, they exhibit form birefringence similar to that of a uniaxial negative crystal. Its optical axis orientation and induced retardance can be controlled by the determination of laser writing parameters. Controllable birefringence with extraordinary thermal stability [3] and reduced chemical durability [4] of nanogratings enabled their application for ultrastable optical data storage, light polarization converters with patterned birefringence and microfluidic circuits [5]. Numerical simulation showed a crucial role of laser-induced defects in launching the self-assembly process [6,7].

Unlike the laser-induced periodic surface structures often referred to as ripples shown to be a universal phenomenon a long time ago [8,9], nanogratings as a bulk modification emerging in the inside of materials were discovered and widely investigated over a decade only in pure and doped fused silica [1,2,5,10]. Later, nanogratings were obtained in vitreous GeO_2 [11,12] and in a number of binary and multicomponent glasses [13–28], including

multicomponent borosilicate Borofloat 33 and BK7 (Corning) [13–15], alkali-free/depleted aluminoborosilicate AF32 (Schott) [14], 7059, Eagle XG (Corning), and soda lime [15] glasses, binary titanium silicate ULE (Corning) [13], Na₂O-SiO₂ [16,17], GeO₂-SiO₂ [18,19], Al₂O₃-SiO₂ [20], Na₂O-GeO₂ [21,22] and ternary Na₂O₃-B₂O₃-SiO₂ [23] glasses. Nanogratings having an atypically large period were recently obtained in borate glasses, namely in sodium borate and sodium aluminoborate systems [24,25]. A specific type of nanograting is based on the laser-induced phase separation process resulting in the precipitation of nanoperoiodical crystalline layers. It was obtained in glasses free of conventional glass-forming oxides: Dy₂O₃-Al₂O₃ [26,27] and La₂O₃-Ta₂O₅-Nb₂O₅ [28] glasses. Similar nanogratings formed by layers of oriented LiNbO₃ nanocrystals were shown in lithium niobium silicate [29,30] and lithium niobium borosilicate [31] glasses. Appearing to be a common phenomenon for oxide dielectrics, nanogratings were also inscribed in single crystals such as quartz [32], sapphire [33] and Nd:YAG [34]. In the case of YAG (Y₃Al₅O₁₂) crystal, their formation was shown to originate from the phase transformation rather than nanopore emergence, and the nanoplanes were formed via Y₃Al₅O₁₂ amorphization or recrystallization into a perovskite-like phase depending on laser writing conditions [34].

In contrast to crystals, glass composition can be varied gradually, which allows for the gradual variation of its properties. Investigation of the effect of glass composition on the formation and properties of nanogratings is now in progress. Some specific compositional and laser exposure parameter effects on nanograting formation in multicomponent glasses [13,15,16,18–22] distinguishing them from fused silica have been revealed but not yet fully explained. Recently, we have shown the formation of nanogratings in a series of binary sodium germanate (SG) glasses containing from 3 to 22 mol.% Na₂O [22]. Interestingly, the formation of nanogratings in 22Na₂O·78GeO₂ glass at the applied laser exposure conditions was accompanied by the precipitation of Na₂Ge₄O₉ microcrystals around them. In the present study, we examined the effect of the laser pulse repetition rate (PRR) on the ultrafast laser-induced modification of 22Na₂O·78GeO₂ glass (hereafter referred to as SG22) in the 50 kHz–1 MHz range.

2. Materials and Methods

Glass under study was fabricated from chemically pure Na₂CO₃ and GeO₂. The batch was molten in a platinum crucible in the electric furnace for 1.5 h at 1100 °C and the melt was quenched between two steel plates. The obtained glass sample had a density equal to 3.94 ± 0.01 g/cm³ and glass transition temperature T_g = 516 °C. More details on its synthesis and characterization were reported earlier [22]. The as-quenched glass was annealed for 8 h at T_g-30 °C and then cut into ~1 mm thick rectangular plane parallel plates, four sides of which were polished to a mirror grade to provide the possibility of top and side view observation.

Pharos SP Yb:KGW-based regeneratively amplified femtosecond laser (Light Conversion Ltd., Vilnius, Lithuania) generating pulses with a variable duration from 180 fs to 10 ps at a tunable PRR up to 1 MHz at 1030 ± 2 nm wavelength was applied for modification of the fabricated glass samples. The sample was positioned using an Aerotech ABL1000 XYZ-motorized air-bearing stage (Aerotech Inc., Pittsburgh, PA, USA). A layout of the setup can be found elsewhere [22]. Sets of dots were written in the glass samples by the stationary laser beam focused into the sample using an Olympus LCPLN50XIR microscope objective (Olympus, Tokyo, Japan) (N.A. = 0.65) at a depth of 50 μm under the glass surface. In the first set of the performed experiments, two pulse energy values within the range based on the previous experiments on SG22 glass [22] were applied: 120 nJ and 210 nJ (if measured at the sample surface), the pulse duration was set to 1.2 ps. The PRR was varied from 67 kHz to 1 MHz. Two mutually orthogonal orientations of the polarization plane of the incident laser beam were used to check the polarization sensitivity of the laser-induced birefringence. In further experiments, we varied the pulse energy from 50 to 250 nJ and the pulse duration from 200 fs to 2 ps. An Olympus BX61 optical microscope (Olympus, Tokyo, Japan) equipped with an Acrio Microbirefringence system (CRi Inc., Woburn, MA,

USA) was used in transmission mode for the observation of the laser-written dots and quantitative birefringence microanalysis in top and side view configurations. Numerical mapping of the orientation of the slow axis of birefringence and the optical phase retardance was performed within the observed area. Confocal Raman spectroscopy of some laser-written domains was performed using a Nanofinder confocal Raman spectrometer included in the NTEGRA Spectra facility (NT-MDT Ltd., Moscow, Russia) using a blue emission line (488 nm wavelength) of an Ar ion laser as an excitation source. Atomic force microscopy (AFM) by means of the NTEGRA Spectra facility was used in the contact mode for visualization of the nanoprecipitated structure of the laser-written nanogratings. To expose cross-sections of the laser-written dots at different depths, a series of birefringent dots was written in the same laser exposure mode with a slight shift of the focusing depth from dot to dot. Then the glass sample was polished to the level of their inscription using an aqueous suspension of CeO₂ powder and then the exposed surface was rinsed with 96 vol.% water solution of ethanol for 1 min according to the sample preparation technique suggested by Wang et al. [21] and used in our previous study [22].

3. Results

The slow axis of birefringence induced in the laser-written dots was perpendicular to the polarization plane of the writing laser beam up to 250 kHz PRR for both pulse energy values applied (Figure 1, top view), which indicated the formation of nanogratings at these conditions. The dots inscribed at a low PRR are not shown in Figure 1 as they look identical to the dots inscribed at 111 kHz in the case of 210 nJ pulses and at 167 kHz in the case of 120 nJ pulses. A side view pseudocolor map of the slow axis of birefringence in Figure 1 highlights only one orientation because in the other case, the optical axis of uniaxial birefringence (fast axis, in this case) is perpendicular to the image plane; thus, it induces no retardance and cannot be detected in this configuration. At higher pulse energy (210 nJ), 250 kHz PRR appears to be very close to the upper limit value of nanograting formation, as only one of two orthogonal orientations of the writing laser beam induced form birefringence.

At higher PRR, the increasing thermal effect of the femtosecond pulses and growing average temperature of the laser-exposed area during the exposure process must have caused glass melting, which prevented the formation of nanogratings. At the same time, ring-shaped birefringent microdomains whose orientation did not correlate with the laser beam polarization plane can be seen in the laser-written dots in the top view configuration starting from 167 kHz at 210 nJ pulse energy (Figure 1a) and from 333 kHz at 120 nJ pulse energy (Figure 1b). These microdomains were found to be Na₂Ge₄O₉ microcrystals, which was confirmed by confocal Raman spectroscopy (Figure 2). The obtained Raman spectra are very similar to those reported for the laser-induced Na₂Ge₄O₉ crystals in SG22 glass [22] and are omitted in this paper. The laser exposure at 1 MHz PRR produced a number of microcracks together with microcrystallization at both pulse energies.

Mapping of the scattering intensity in the Raman shift range of 510–575 cm⁻¹ including the dominant Raman peak of Na₂Ge₄O₉ crystal showed that the crystallized regions had the shape of a tube with a circular cross-section oriented along the beam propagation direction. The peripheral character of crystallization was also confirmed by the AFM images (Figure 3). The ring-shaped bulge at the exposed surface (Figure 3b,c) corresponds to the cross-section of the crystallized region, which appears to be more durable to polishing or to liquid etching than surrounding glass [22]. The width of the crystalline layer varied from 0.4 μm to 0.8 μm for the given laser writing mode according to the AFM images. The lateral precipitation of the crystalline phase relative to the laser beam propagation axis is typical for ultrafast laser-induced crystallization, which is known to start at the boundary of glass and liquid [35]. The PRR range as high as hundreds of kHz is also considered desirable to provide sufficient average temperature for microcrystal growth under the pulses with tens to hundreds of nJ of energy, though at higher pulse energy, crystal growth can be launched even below 10 kHz PRR [36]. It should be noted that at a

low repetition rate (Figure 1a, 111–143 kHz), regions with form birefringence induced by 210 nJ pulses are longer, whereas at a higher repetition rate, form birefringence appeared in the upper part of the laser-modified region, farther from the focal point. At the same time, crystallization took place in its lower part, closer to the focal point. A crystallized domain and a nanograting showed only partial overlapping along the beam propagation direction, i.e., along the vertical axis in our case (Figure 3). Evidently, in the latter case, the higher laser beam intensity near the focal point induces glass melting, while at the opposite edge of the modified region, the glass viscosity is still large enough to keep the emerging self-assembled structure of the nanograting.

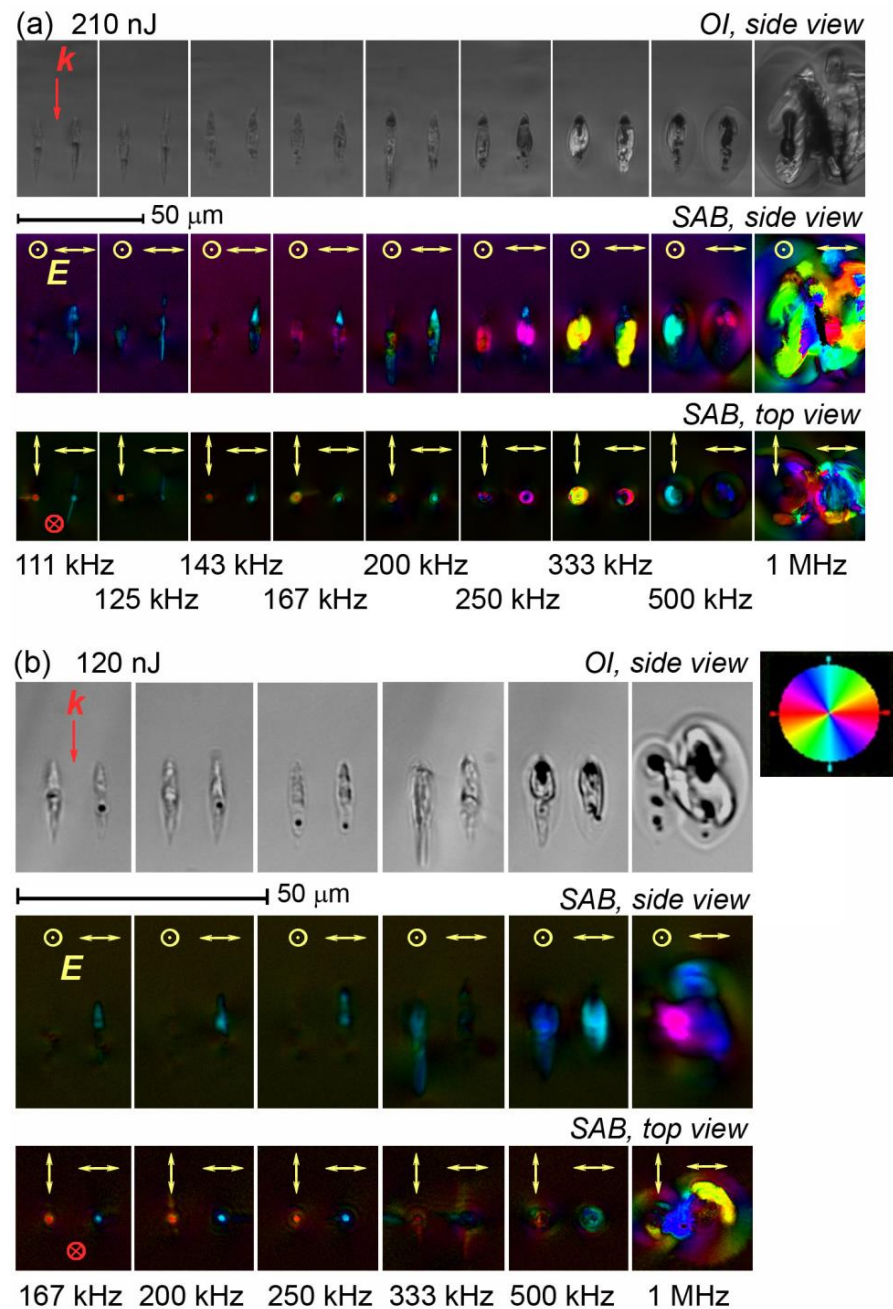


Figure 1. Brightfield optical images (OI) of the side view and pseudocolor maps of the orientation of the slow axis of birefringence (SAB) of the dots written in SG22 glass by 10^6 laser pulses per dot at the pulse duration of 1.2 ps and the pulse energy of 210 nJ (a) and 120 nJ (b) and the varied PRR and polarization plane orientation E (indicated in yellow). The notation k (indicated in red) is for the wave vector direction.

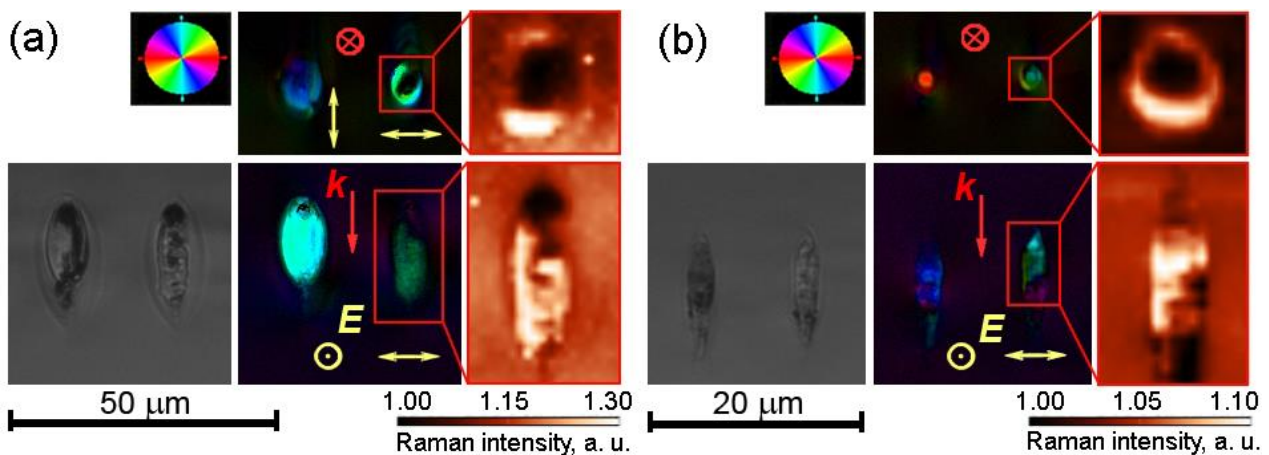


Figure 2. Brightfield OI of side view, pseudocolor maps of the orientation of SAB and Raman maps of nanogratings inscribed in GS22 glass by $5 \cdot 10^5$ laser pulses with 210 nJ energy at the PRR of 333 kHz (a) and 200 kHz (b). Top view and side view are shown in the upper and lower rows, respectively. Brightness shows the area under Raman spectra in the $510\text{--}575\text{ cm}^{-1}$ range, including the strongest characteristic peak of $\text{Na}_2\text{Ge}_4\text{O}_9$ crystalline phase. k and E indicate writing laser beam propagation direction and polarization plane orientation, respectively.

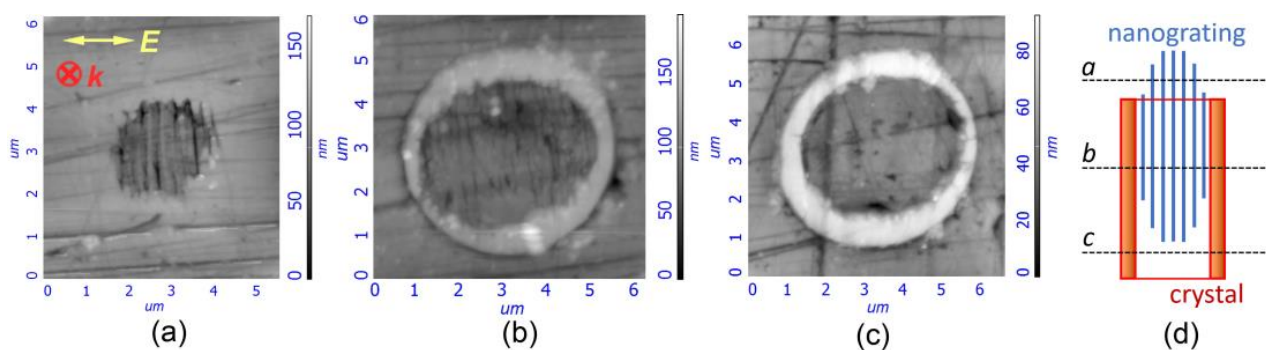


Figure 3. AFM images of the cross-sections of the laser-written birefringent microdomains exposed at a different depth and showing a nanograting (a), a nanograting surrounded by crystals (b) and a crystalline ring without a nanograting inside it (c). A scheme of the cross-section locations relative to the laser-written dot (d). The images are acquired from different microdomains written at the same conditions by 10^6 pulses having 210 nJ energy, 1.2 ps duration and 143 kHz PRR. k and E indicate writing laser beam propagation direction and polarization plane orientation, respectively, and are the same for images (a–c).

A detailed quantitative analysis of the laser-induced form birefringence in fused silica, some commercial multicomponent glasses (Schott Borofloat 33, Corning ULE) and vitreous GeO_2 subjected to the PRR performed by Lancry et al. [37] revealed a monotonous fall of retardance. It gradually accelerated, with PRR starting from 50 to 100 kHz for fused silica and ULE, or from 10 kHz for lower-melting Borofloat 33 and GeO_2 , whereas lower PRR had no effect on the retardance. This was explained by a decrease in the number of pores forming nanoplanes in the nanogratings due to the viscoelastic flow of glass occurring when averaged laser processing temperatures approached the glass softening point. A similar trend was shown by Xie et al. [15] using the example of Borofloat 33 glass in the 10–1000 kHz PRR range and in the full range of pulse energy corresponding to nanograting formation. It was also demonstrated that the lower pulse energy threshold of nanograting formation was independent of the PRR. However, the pulse energy window allowing for nanograting formation gradually decreased with a PRR due to the increase in the thermal effect of laser pulses. The similar pulse energy window behavior was described in detail

for nanogratings inscribed in fused silica [38]. In our case, the retardance measured in fused silica remained independent of the PRR up to 500 kHz, likely because of much smaller pulse energy (120 or 210 nJ vs. 1 μ J pulses applied by Lancry et al. [37] at similar focusing conditions) and a less pronounced thermal effect. However, the retardance of the laser-written birefringent domains in SG22 glass, though constant at a low PRR, manifested an unexpected substantial increase with the PRR starting from 110 to 125 kHz (Figure 4), which appears to contradict the abovementioned data reported for various glasses [37]. Data obtained for form birefringence inscribed by 120 nJ and 210 nJ pulses show that higher pulse energy evidently induces an increase in retardance starting from a lower PRR.

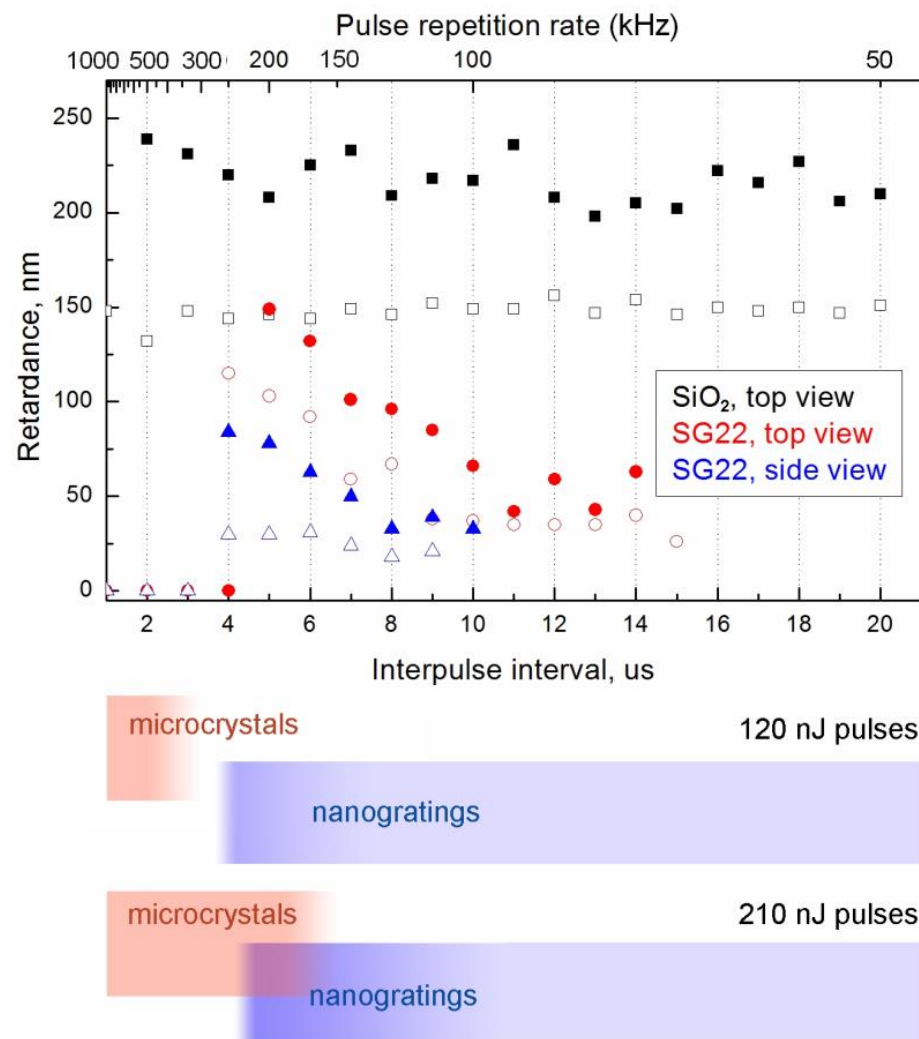


Figure 4. Retardance of nanogratings written by 10^6 pulses per dot in SG22 glass at 1.2 ps pulse duration, and 120 nJ (\circ —top view, \triangle —side view) and 210 nJ (\bullet —top view, \blacktriangle —side view) pulse energy and in SiO₂ glass (top view) at 120 nJ (\square) and 210 nJ (\blacksquare) pulse energy as a function of PRR (top). Diagram of the nanograting formation and crystallization at an indicated pulse energy and the same PRR scale (bottom).

To check the effect of the retardance increase in the nanogratings starting from a certain PRR of the beam used for their inscription across a wider pulse energy range, a set of birefringent dots was written by 10^6 pulses with a 1.2 ps duration and energy varying from 50 to 260 nJ (Figure 5). The accelerating growth of the retardance in the birefringent dots starting from a certain PRR level can be observed at all applied pulse energy values. The corresponding threshold interpulse interval grows monotonously and almost linearly with the pulse energy in the examined range. An instability of retardance at

high PRR values corresponding to 2 μs and 3 μs interpulse interval is related to the strong contribution of crystal- and stress-related birefringence together with the degradation of nanogratings. Obviously, the domains written at 500 kHz PRR (2 μs interpulse interval) contain nanogratings only in the case of the relatively low pulse energies of 50 nJ and 80 nJ.

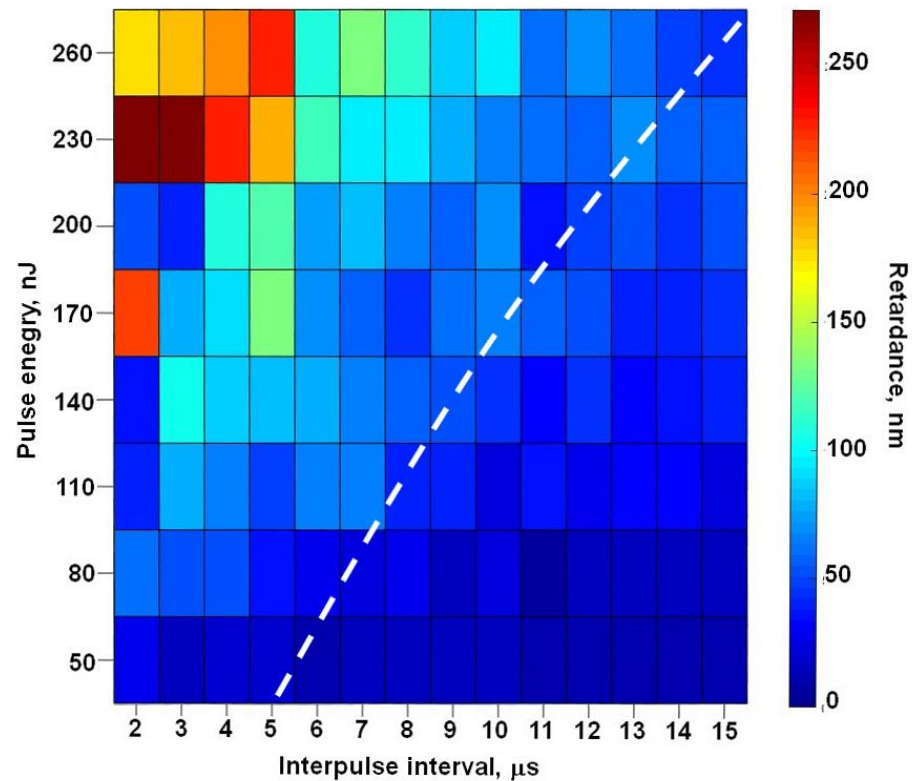


Figure 5. A pseudocolor chart of the retardance in birefringent domains written in SG22 glass by 10^6 laser pulses of 1.2 ps duration as a function of the pulse energy and the interpulse interval. The white dashed line indicates an approximate boundary at which the measured retardance starts growing over its initial level independent of PRR.

We have also analyzed the dependence of retardance of nanogratings inscribed in SG22 glass on the pulse duration. A 2D pseudocolor plot of retardance in nanogratings written in SG22 glass by and 10^6 pulses per dot at 210 nJ pulse energy as a function of the pulse duration and the PRR is given in Figure 6. Importantly, an earlier reported [22] sharp pulse duration threshold occurs fully independent of the PRR in the range corresponding to the nanograting formation. The dependence of retardance on the pulse duration, including its fast rise until ~ 1 ps and further slow fall, is most pronounced for the high retardance obtained at 200 kHz PRR, which also conforms to the previously published data [22]. The slow fall of retardance with the pulse duration for the pulses longer than ~ 1.2 ps is related to the reduction in the peak intensity of longer laser pulses at the constant pulse energy obviously resulting from a lower nonlinear absorption rate. A similar trend can be observed in the data earlier reported for nanogratings in other glasses, including fused silica, AF32 and Borofloat33 [14].

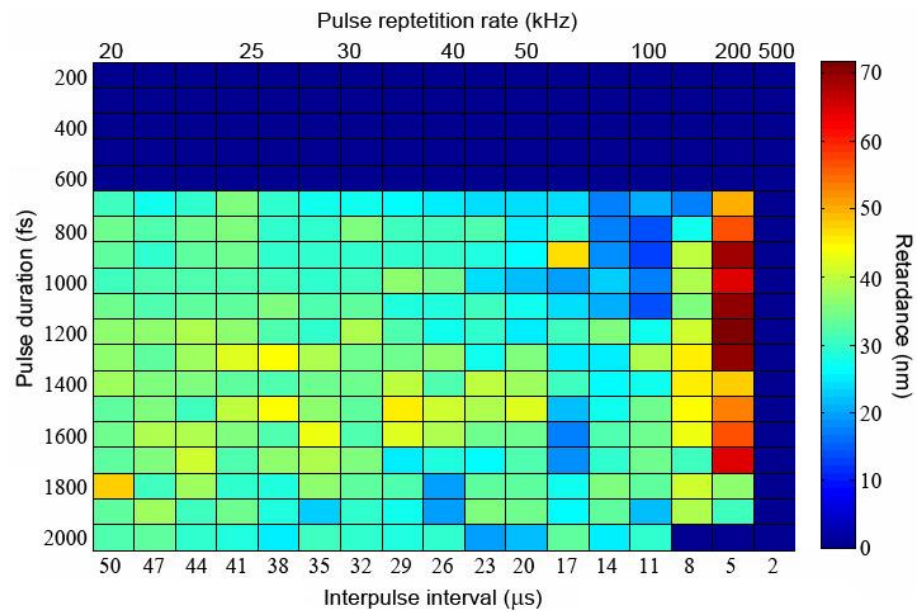


Figure 6. Pseudocolor chart of retardance in nanogratings laser-written in SG22 glass using 10^6 pulses per dot at 210 nJ pulse energy as a function of pulse duration and PRR.

4. Discussion

To explain the unexpected effect of retardance growth with the PRR in the laser-written nanogratings in SG22 glass, earlier reported data on redistribution of alkali cations during the inscription of nanogratings in $15\text{Na}_2\text{O}\cdot 85\text{SiO}_2$ glass are helpful [17]. The formation of those nanogratings using 10^6 – 10^7 pulses with 600 fs duration at 200 kHz PRR was accompanied by the migration of most of Na^+ cations out of the nanograting driven by the thermal diffusion (also known as Soret effect [39]). The rest of the Na^+ was concentrated in the nanoplanes, giving rise to the precipitation of $\text{Na}_2\text{Si}_4\text{O}_9$ nanocrystals. In the germanate glass matrix, the migration of Na^+ cations out of the focal area of the stationary ultrafast laser beam due to thermal diffusion in the germanate glass matrix was demonstrated for $15\text{Na}_2\text{O}\cdot 85\text{GeO}_2$ glass exposed to 1.4 μJ pulses at 250 kHz PRR [40]. The effect of a nanoperiodical redistribution of remaining sodium into nanoplanes within nanogratings written in SG22 glass can also be expected from the analogy with sodium silicate glass.

Moreover, the higher the content of alkaline oxide in binary silicate [16] or germanate [22] glass, the higher the number of pulses required to induce form birefringence and, in the case of sodium germanate glasses [22], the lower retardance achieved, other conditions being equal. Therefore, sodium depletion inside the nanograting was expected to increase with the PRR due to the intensification of thermal diffusion, when the thermal effect of the laser pulses emerged. A corresponding shift of glass composition in the nanograting to the higher content of GeO_2 meant the possibility to achieve higher retardance under the same exposure conditions. It should be mentioned that the retardance behavior at various PRR levels reported earlier for various glasses [15,37] was studied in nanogratings written by the moving laser beam at scanning speeds providing 10^3 pulses/ μm overlapping rate. Thus, depending on the pulse energy, the total incident light energy dose applied in those studies occurred to be two or three orders of magnitude lower than in the present experiments in SG22 glass where dots were written by $5\cdot 10^5$ or 10^6 pulses. This can be another reason for such a significant difference in retardance trends, because the introduced energy dose must have been too small for glass composition shift and possible compositional effects on retardance, even in the case of Borofloat 33 glass that contains relatively mobile alkaline ions [37]. In contrast, the total dose of the incident light energy applied for a vivid demonstration of significant sodium migration out of the irradiated area of sodium germanate glass [40] was by two orders of magnitude higher in our case, though less tight focusing partially compensated this difference in terms of the area density of this dose.

Though the role of nanoperiodical alkali cation redistribution inside a nanograting in the rise of form birefringence is not well understood so far, it can also be assumed to give a contribution into the nanoperiodical refractive index contrast providing form birefringence of the nanograting. This cation redistribution process, which can be regarded as a kind of regular phase separation, is also expected to be enhanced by the thermal action of femtosecond pulses, since an increase in the time-averaged temperature facilitates the diffusion of cations. If this contribution into the refractive index contrast is positive in the case of SG22 glass, this can be another reason giving rise to the unusual growth in the laser-induced retardance with the PRR of the writing laser beam.

Significantly, qualitative evaluation of form birefringence in unconventional glasses [27,28] revealed a PRR threshold of about 100 kHz or higher depending on the pulse energy. Below this threshold, crystallized nanogratings cannot be formed due to the necessity of the thermal effect of the ultrafast laser beam for phase separation and nanocrystallization. This principally distinguishes them from nanopore-based, fully amorphous nanogratings in fused silica, ULE glass or Borofloat 33 glass [13,35], which manifest no low PRR threshold for nanograting inscription. Nanogratings formed in SG22 glass could occur in an intermediate case between these two utmost kinds of nanograting realization. The contribution of different mechanisms to a raise of form birefringence in them probably varies depending on the beam parameters. Further detailed analysis of their morphology and elemental distribution is required to confirm this assumption and explain the revealed features.

5. Conclusions

In conclusion, ultrafast laser-induced micromodification of $22\text{Na}_2\text{O}\cdot 78\text{GeO}_2$ glass including nanograting formation and microcrystallization is examined and an unexpected PRR effect on ultrafast-laser nanostructuring of $22\text{Na}_2\text{O}\cdot 78\text{GeO}_2$ glass is demonstrated. At a lower PRR (≤ 250 kHz), the inscription of nanogratings possessing form birefringence is observed under series of 10^5 – 10^6 pulses, whereas a higher PRR launches peripheral microcrystallization with precipitation of $\text{Na}_2\text{Ge}_4\text{O}_9$ due to the thermal effect of femtosecond pulses. Depending on the laser pulse energy, the PRR ranges corresponding to nanograting formation and crystallization can overlap or be separated from each other. We revealed the unusual growth of optical retardance of the laser-written nanogratings with the PRR, starting from a threshold value with an order of magnitude of $\sim 10^2$ kHz and inversely proportional to the pulse energy, varying from 67 to 200 kHz in the studied range of the pulse energy. This growth gradually accelerates with the pulse repetition rate until the thermal effect of laser pulses is too large for nanograting formation due to glass melting. The optical retardance increase occurs whether crystallization around the nanograting is induced or not and distinguishes the investigated glass from fused silica and some multicomponent glasses studied earlier, which manifest stability or a monotonous decrease in retardance in nanogratings with the PRR. The observed phenomenon is likely related to the thermal diffusion of sodium cations rising with the thermal effect of the laser beam when the thermal effect of the ultrashort laser pulses becomes noticeable.

Author Contributions: Conceptualization, S.V.L. and V.N.S.; methodology, S.S.F. and A.S.L.; software, S.S.F.; validation, A.I.P. and A.S.L.; investigation, A.I.P., S.S.F. and S.V.L.; writing—original draft preparation, S.V.L.; writing—review and editing, S.S.F., A.S.L. and V.N.S.; visualization, S.V.L. and S.S.F.; supervision, V.N.S.; project administration, S.V.L.; funding acquisition, S.V.L. All authors have read and agreed to the published version of the manuscript.

Funding: This research was funded by the Russian Foundation for Basic Research, grant number 21-53-12026.

Data Availability Statement: Not applicable.

Conflicts of Interest: The authors declare no conflict of interest.

References

1. Shimotsuma, Y.; Kazansky, P.G.; Qiu, J.; Hirao, K. Self-organized nanogratings in glass irradiated by ultrashort light pulses. *Phys. Rev. Lett.* **2003**, *91*, 247405. [[CrossRef](#)] [[PubMed](#)]
2. Canning, J.; Lancry, M.; Cook, K.; Weickman, A.; Brisset, F.; Poumellec, B. Anatomy of a femtosecond laser processed silica waveguide. *Opt. Mater. Express* **2011**, *1*, 998–1008. [[CrossRef](#)]
3. Bricchi, E.; Kazansky, P.G. Extraordinary stability of femtosecond direct written structures. *Appl. Phys. Lett.* **2006**, *88*, 111119. [[CrossRef](#)]
4. Hnatovsky, C.; Taylor, R.S.; Simova, E.; Rajeev, P.P.; Rayner, D.M.; Bhardwaj, V.R.; Corkum, P.B. Fabrication of microchannels in glass using focused femtosecond laser radiation and selective chemical etching. *Appl. Phys. A* **2006**, *84*, 47–61. [[CrossRef](#)]
5. Zhang, B.; Liu, X.; Qiu, J. Single femtosecond laser beam induced nanogratings in transparent media—Mechanisms and applications. *J. Materiomics* **2019**, *5*, 1–14. [[CrossRef](#)]
6. Rudenko, A.; Colombier, J.P.; Itina, T. From random inhomogeneities to periodic nanostructures induced in bulk silica by ultrashort laser. *Phys. Rev. B* **2016**, *93*, 075427. [[CrossRef](#)]
7. Rudenko, A.; Colombier, J.-P.; Itina, T.E.; Stoian, R. Genesis of nanogratings in silica bulk via multipulse interplay of ultrafast photo-excitation and hydrodynamics. *Adv. Opt. Mater.* **2021**, *9*, 2100973. [[CrossRef](#)]
8. Van Driel, H.M.; Sipe, J.E.; Young, J.F. Laser-Induced Periodic Surface Structure on Solids: A Universal Phenomenon. *Phys. Rev. Lett.* **1982**, *49*, 1955. [[CrossRef](#)]
9. Bonse, J.; Kirner, S.V.; Krüger, J. Laser-Induced Periodic Surface Structures (LIPSS). In *Handbook of Laser Micro-and Nano-Engineering*; Sugioka, K., Ed.; Springer: Cham, Switzerland, 2021. [[CrossRef](#)]
10. Lancry, M.; Poumellec, B.; Chahid-Erraji, A.; Beresna, M.; Kazansky, P.G. Dependence of the femtosecond laser refractive index change thresholds on the chemical composition of doped-silica glasses. *Opt. Mater. Express* **2011**, *1*, 711–723. [[CrossRef](#)]
11. Zhang, F.; Zhang, H.; Dong, G.; Qiu, J. Embedded nanogratings in germanium dioxide glass induced by femtosecond laser direct writing. *J. Opt. Soc. Am. B* **2014**, *31*, 860–864. [[CrossRef](#)]
12. Zhang, F.; Cerkauskaite, A.; Drevinskas, R.; Kazansky, P.G.; Qiu, J. Microengineering of optical properties of GeO₂ glass by ultrafast laser nanostructuring. *Adv. Opt. Mater.* **2017**, *5*, 1700342. [[CrossRef](#)]
13. Richter, S.; Miese, C.; Döring, S.; Zimmermann, F.; Withford, M.J.; Tünnermann, A.; Nolte, S. Laser induced nanogratings beyond fused silica—Periodic nanostructures in borosilicate glasses and ULE™. *Opt. Mater. Express* **2013**, *3*, 1161–1166. [[CrossRef](#)]
14. Fedotov, S.S.; Drevinskas, R.; Lotarev, S.V.; Lipatiev, A.S.; Beresna, M.; Čerkauskaitė, A.; Sigaev, V.N.; Kazansky, P.G. Direct writing of birefringent elements by ultrafast laser nanostructuring in multicomponent glass. *Appl. Phys. Lett.* **2016**, *108*, 071905. [[CrossRef](#)]
15. Xie, Q.; Cavillon, M.; Pugliese, D.; Janner, D.; Poumellec, B.; Lancry, M. On the formation of nanogratings in commercial oxide glasses by femtosecond laser direct writing. *Nanomaterials* **2022**, *12*, 2986. [[CrossRef](#)]
16. Fedotov, S.S.; Lipat'ev, A.S.; Lotarev, S.V.; Sigaev, V.N. Local formation of birefringent structures in alkali silicate glass by femtosecond laser beam. *Glass Ceram.* **2017**, *74*, 227–229. [[CrossRef](#)]
17. Lotarev, S.; Fedotov, S.; Lipatiev, A.; Presnyakov, M.; Kazansky, P.; Sigaev, V. Light-driven nanopositional modulation of alkaline cation distribution inside sodium silicate glass. *J. Non-Cryst. Solids* **2018**, *479*, 49–54. [[CrossRef](#)]
18. Zimmermann, F.; Lancry, M.; Plech, A.; Richter, S.; Hari Babu, B.; Poumellec, B.; Tünnermann, A.; Nolte, S. Femtosecond laser written nanostructures in Ge-doped glasses. *Opt. Lett.* **2016**, *41*, 1161–1164. [[CrossRef](#)]
19. Lancry, M.; Canning, J.; Cook, K.; Heili, M.; Neuvill, D.R.; Poumellec, B. Nanoscale femtosecond laser milling and control of nanoporosity in the normal and anomalous regimes of GeO₂-SiO₂ glasses. *Opt. Mater. Express* **2016**, *6*, 321–330. [[CrossRef](#)]
20. Wang, Y.; Wei, S.; Cicconi, M.R.; Tsuji, Y.; Shimizu, M.; Shimotsuma, Y.; Miura, K.; Peng, G.-D.; Neuvill, D.R.; Poumellec, B.; et al. Femtosecond laser direct writing in SiO₂-Al₂O₃ binary glasses and thermal stability of Type II permanent modifications. *J. Am. Ceram. Soc.* **2020**, *103*, 4286–4294. [[CrossRef](#)]
21. Wang, J.; Liu, X.; Dai, Y.; Wang, Z.; Qiu, J. Effect of sodium oxide content on the formation of nanogratings in germanate glass by a femtosecond laser. *Opt. Express* **2018**, *26*, 12761–12768. [[CrossRef](#)]
22. Lotarev, S.V.; Fedotov, S.S.; Kurina, A.I.; Lipatiev, A.S.; Sigaev, V.N. Ultrafast laser-induced nanogratings in sodium germanate glasses. *Opt. Lett.* **2019**, *44*, 1564–1567. [[CrossRef](#)]
23. Lotarev, S.V.; Lipat'iev, A.S.; Fedotov, S.S.; Mikhailov, A.A.; Sigaev, V.N. Laser writing of polarization-sensitive birefringence in sodium-borosilicate glasses. *Glass Ceram.* **2019**, *76*, 85–88. [[CrossRef](#)]
24. Fedotov, S.S.; Lipatiev, A.S.; Lipateva, T.O.; Lotarev, S.V.; Mel'nikov, E.; Sigaev, V.N. Femtosecond laser-induced birefringent microdomains in sodium-borate glass for highly secure data storage. *J. Am. Ceram. Soc.* **2021**, *104*, 4297–4303. [[CrossRef](#)]
25. Fedotov, S.S.; Lipat'ev, A.S.; Lipat'eva, T.O.; Lotarev, S.V.; Prikhach, N.K.; Sigaev, V.N. Polarization-dependent birefringence in sodium aluminoborate glasses. *Glass Ceram.* **2022**, *79*, 85–87. [[CrossRef](#)]
26. Mori, S.; Kurita, T.; Shimotsuma, Y.; Sakakura, M.; Kiyotaka, M. Nanogratings embedded in Al₂O₃-Dy₂O₃ glass by femtosecond laser irradiation. *J. Laser Micro/Nanoeng.* **2016**, *11*, 87–90. [[CrossRef](#)]
27. Shimotsuma, Y.; Mori, S.; Nakanishii, Y.; Kim, E.; Sakakura, M.; Miura, K. Self-assembled glass/crystal periodic nanostructure in Al₂O₃-Dy₂O₃ binary glass. *Appl. Phys. A* **2018**, *124*, 82. [[CrossRef](#)]
28. Zhang, B.; Tan, D.; Liu, X.; Tong, L.; Kazansky, P.G.; Qiu, J. Self-organized periodic crystallization in unconventional glass created by an ultrafast laser for optical attenuation in the broadband near-infrared region. *Adv. Opt. Mater.* **2019**, *7*, 1900593. [[CrossRef](#)]

29. Cao, J.; Mazerolles, L.; Lancry, M.; Solas, D.; Brisset, F.; Poumellec, B. Form birefringence induced in multicomponent glass by femtosecond laser direct writing. *Opt. Lett.* **2016**, *41*, 2739–2742. [[CrossRef](#)] [[PubMed](#)]
30. Cao, J.; Poumellec, B.; Mazerolles, L.; Brisset, F.; Helbert, A.; Surble, S.; He, X.; Lancry, M. Nanoscale phase separation in lithium niobium silicate glass by femtosecond laser irradiation. *J. Am. Ceram. Soc.* **2017**, *100*, 115–124. [[CrossRef](#)]
31. Muzi, E.; Cavillon, M.; Lancry, M.; Brisset, F.; Sapaly, B.; Janner, D.; Poumellec, B. Polarization-oriented LiNbO₃ nanocrystals by femtosecond laser irradiation in LiO₂–Nb₂O₅–SiO₂–B₂O₃ glasses. *Opt. Mater. Express* **2021**, *11*, 1313–1320. [[CrossRef](#)]
32. Zhang, F.; Nie, Z.; Huang, H.; Ma, L.; Tang, H.; Hao, M.; Qiu, J. Self-assembled three-dimensional periodic micro-nano structures in bulk quartz crystal induced by femtosecond laser pulses. *Opt. Express* **2019**, *27*, 6442–6450. [[CrossRef](#)]
33. Zhai, Q.; Ma, H.; Lin, X.; Li, Y.; Yin, W.; Tang, X.; Dai, Y. Evolution of self-organized nanograting from the pre-induced nanocrack-assisted plasma–laser coupling in sapphire. *Appl. Phys. B* **2021**, *127*, 74. [[CrossRef](#)]
34. Lipateva, T.O.; Lipatiev, A.S.; Karateev, I.V.; Okhrimchuk, A.G.; Fedotov, S.S.; Lotarev, S.V.; Alagashev, G.K.; Sigaev, V.N. Direct laser writing in YAG single crystal: Evolution from amorphization to nanograting formation and phase transformation. *J. Alloys Compounds* **2023**, *942*, 169081. [[CrossRef](#)]
35. Stone, A.; Sakakura, M.; Shimotsuma, Y.; Miura, K.; Hirao, K.; Dierolf, V.; Jain, H. Femtosecond laser-writing of 3D crystal architecture in glass: Growth dynamics and morphological control. *Mater. Des.* **2018**, *146*, 228–238. [[CrossRef](#)]
36. Lipateva, T.O.; Lotarev, S.V.; Lipatiev, A.S.; Kazansky, P.G.; Sigaev, V.N. Formation of crystalline dots and lines in lanthanum borogermanate glass by the low pulse repetition rate femtosecond laser. *SPIE Proc.* **2015**, *9450*, 945018. [[CrossRef](#)]
37. Lancry, M.; Zimmerman, F.; Desmarchelier, R.; Tian, J.; Brisset, F.; Nolte, S.; Poumellec, B. Nanogratings formation in multicomponent silicate glasses. *Appl. Phys. B* **2016**, *122*, 66. [[CrossRef](#)]
38. Richter, S.; Heinrich, M.; Döring, S.; Tünnermann, A.; Nolte, S. Formation of femtosecond laser-induced nanogratings at high repetition rates. *Appl. Phys. A* **2011**, *104*, 503–507. [[CrossRef](#)]
39. Shimizu, M. Soret effect in binary glass-forming oxide melts: Theory and its verification. *J. Ceram. Soc. Jpn.* **2019**, *127*, 507–513. [[CrossRef](#)]
40. Wang, X.; Sakakura, M.; Liu, Y.; Qiu, J.; Shimotsuma, Y.; Hirao, K.; Miura, K. Modification of long range order in germanate glass by ultra fast laser. *Chem. Phys. Lett.* **2011**, *511*, 266–269. [[CrossRef](#)]

Disclaimer/Publisher’s Note: The statements, opinions and data contained in all publications are solely those of the individual author(s) and contributor(s) and not of MDPI and/or the editor(s). MDPI and/or the editor(s) disclaim responsibility for any injury to people or property resulting from any ideas, methods, instructions or products referred to in the content.